Lab on a Chip

Accepted Manuscript

ROYAL SOCIETY OF CHEMISTRY

www.rsc.org/loc

A table of contents entry

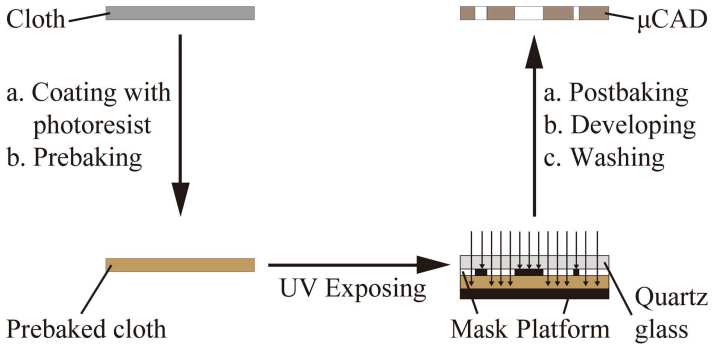

Simple, low-cost and high-throughput fabrication of microfluidic cloth-based analytical devices (μCADs) using a photolithographical patterning technique

Low-cost, high-throughput fabrication of cloth-based microfluidic devices using a photolithographical patterning technique

Peijing Wu, Chunsun Zhang*

MOE Key Laboratory of Laser Life Science & Institute of Laser Life Science, College of Biophotonics, South China Normal University, Guangzhou 510631, China

*** The contact information of the corresponding authors is**:

Chunsun Zhang, PhD, Professor

MOE Key Laboratory of Laser Life Science & Institute of Laser Life Science,

College of Biophotonics, South China Normal University,

No.55, Zhongshan Avenue West, Tianhe District,

Guangzhou, 510631,

P.R. China

Tel: +86-20-85217070-8501, Fax: +86-20-85216052

E-mail: zhangcs@scnu.edu.cn; zhangcs_scnu@126.com

Abstract

In this work, we first report a facile, low-cost and high-throughput method for photolithographical fabrication of microfluidic cloth-based analytical devices (μCADs) by simply using the cotton cloth as substrate material and employing inexpensive hydrophobic photoresist laboratory-formulated from commercially available reagents, which allows patterning of reproducible hydrophilic-hydrophobic features in cloth with well-defined and uniform boundaries. Firstly, we evaluated the wicking property of cotton cloths by testing the wicking rate in the cloth channel, in combination with scanning electron microscopy (SEM) and energy dispersive spectroscopy (EDS) analyses. It is demonstrated that the wicking property of the cloth microfluidic channel can be improved by soaking cloth substrate in 20 wt% NaOH solution and by washing cloth-based microfluidic patterns with 3 wt% SDS solution. Next, we studied the minimum dimensions achievable for the width of hydrophobic barriers and hydrophilic channels. The results indicate that the smallest width for a desired hydrophobic barrier is designed to be 100 μm and that for a desired hydrophilic channel is designed to be 500 μm. Finally, the high-throughput μCADs prepared using the developed fabrication technique were demonstrated for colorimetric assays of glucose and protein in artificial urine samples. It has been shown that the photolithographically patterned μCADs have the potential for simple, quantitative colorimetric urine test. The combination of cheap cloth and inexpensive high-throughput photolithography enables the development of new types of low-cost cloth-based microfluidic devices, such as “microzone plates” and “gate arrays”, which provide new methods to perform biochemical assays or control fluid flow.

1. Introduction

The detection of analytes such as nucleic acids, proteins, drugs and metabolites in body fluids, and other biochemical fluids is essential for a series of applications including medical diagnostics, environmental monitoring, food safety testing and forensic analysis. Rapid, inexpensive, accurate point-of-care testing (POCT) [**1**] of such analytes has gained increasing international attention, especially in developing regions or in resource-limited settings. However, most of conventional systems designed for POCT applications often suffer several drawbacks such as the need for professional operation, high costs, bulkiness, heaviness and delayed output of test results. Therefore, there is a great need for those systems that are inexpensive, portable, easy-to-operate, and capable of performing rapid and sensitive detection. Over the past few years, paper-based microfluidic analytical devices (μPADs) [**2-4**], in which aqueous solutions wick through a porous matrix of hydrophilic cellulose fibers delimited by hydrophobic barriers, have gained prominence as solutions to this problem.

As part of a continuous effort to explore new materials for making simple, low-cost analytical devices, threads and cloths have been investigated as inexpensive materials for fabrication of disposable microfluidic devices [**5**]. Up to now, a variety of methods have been reported in the literature for fabrication of thread- or cloth-based microfluidic analytical devices (μTADs or μCADs). The majority of hydrophilic wicking channels have been created by two effective manufacturing techniques. The first involves the use of hydrophilic threads and yarns to construct microfluidic channels [**6-19**]. An obvious advantage of thread-based microfluidic channel over a paper-based one is that the former does not require hydrophobic barriers to define channels. In addition, thread can easily be wound, woven and knotted to

fabricate different functional fluidic elements such as mixers [**13**], splitters [**16**], serial dilutor [**16**] and sampling with variable volume injection [**18**]. However, this fabrication method of μTADs still has some inherent difficulties to be used for mass production of the devices, as well as for determining the exact detection zones in the case of μTADs.

The second technique of making hydrophilic wicking channels involves the use of hydrophilic woven cloths. In 2011, Bhandari et al. first introduced woven fabric as a substrate for microfluidic devices [**20**]. They utilized a conventional weaving technique to fabricate a cloth-based microfluidic immunoassay sensor, where silk yarns with different wicking properties were used to form strip-control units in cloth. Similarly, Owens et al. employed hydrophilic poly(ethylene terephthalate) (PET) and hydrophobic polypropylene (PP) yarns to systematically construct woven textile fabric to create amphiphilic microchannels with defined orientations and locations [**21**]. As a result, simultaneous wicking of immiscible liquids into the hydrophilic and hydrophobic microchannels of an amphiphilic fabric was demonstrated. Using flexible textile PET/PP materials, the preprogrammed yarn-based weaving and the yarn-selective surface modification method were coupled to fabricate microfluidic fiber channels with switchable water transport [**22**]. In all the above-mentioned woven cloth-based microfluidic devices, the desired detection zones are still difficult to be exactly controlled. In addition, complicated two-dimensional (2-D) structures or three-dimensional (3-D) μCADs are difficulty to be created. In order to overcome some of these problems, Nilghaz et al. have developed a wax patterning technique for fabrication of flexible 2-D and 3-D μCADs [**23**]. Very recently, both works on μCAD made by wax-patterning [**24, 25**] have proven that μCADs can do quantitative electrochemical assay or

enzyme-linked immunosorbent assay (ELISA) with more complexity compared to when it was first proposed [**23**]. In this wax-patterning technique, the fabrication process included as follows. The printed paper was immersed in the hot wax to suck it up, and then the hydrophilic parts were punched out from the paper. Next, this wax-impregnated paper was fixed on the cloth to transfer the wax from paper to cloth by heat treatment. After wax transfer to cloth, the paper was removed from the cloth, resulting in a 2-D μCAD. To fabricate 3-D μCADs, a single layer of wax-patterned cloth could be folded along a predefined folding line and subsequently pressed using mechanical force. The developed fabrication approach has some advantages such as having specific detection zones as well as being more compact and embeddable. However, the designed pattern in this approach may be difficult to be accurately carved on wax-impregnated paper, especially by a handheld cutter blade. In addition, the fabrication speed, throughput and accuracy are dependent on the carving process to a certain extent.

In industry and basic research, the photo- or UV-lithography is most commonly used method as it is fast (parallel exposure) and well-controlled, allows fabrication of very small, high-throughput patterns on a suitable surface, and can achieve very high structural resolution. Since Whitesides and co-workers pioneered the field by patterning chromatography paper via photolithography in 2007 [**2**], the photolithography has been explored by many research groups to fabricate the paper-based microfluidic devices [**26-51**]. In most works on patterning paper using photolithography, paper was first soaked in SU-8 photoresist and then exposed to UV light through a mask defining the shape of the hydrophobic regions, followed by removing the SU-8 photoresist from the unexposed areas revealing the original paper

structures [**2**, **26**, **27**, **29**, **32-34, 37, 39**, **40**, **42**, **43**, **45**, **46**, **48-51**]. SU-8 is a relatively simple mixture, but its cost as a commercial photoresist is very high and as a result the fabrication of SU-8-patterned paper device is much expensive. To reduce the cost of fabrication, some less-expensive alternative photoactive polymers to SU-8 have been reported for photolithographic fabrication of paper-based device, such as polymer mixture of Zipcone UA and Norland Optical Adhesive 74 [**38**], SC (cyclized poly(isoprene) derivative) [**27**], or laboratory-formulated epoxy-based negative photoresist with similar properties to SU-8 [**27**, **44**, **49**]. Recently, two prominent works on coupling silane to paper fibers, followed by UV-lithography of the corresponding coating, have been reported for fabrication of μPADs [**28**, **36**]. In addition, Haller et al. patterned chromatography papers via photoinduced chemical vapor-phase grafting of hydrophobic photoresponsive poly(o-nitrobenzyl methacrylate) (PoNBMA) to the paper fibers, followed by UV-lithography of the PoNBMA coating through a photomask [**35**]. All the aforementioned photolithographic fabrication methods can create a certain μPAD for specific sensing applications. To the best of our knowledge, however, no work on patterning cloth by photolithography has been reported.

In 1954, the Eastman Kodak company synthesized the first photosensitive polymer-poly(vinyl cinnamate) (PVC) in human history [**52**]. Since that time, the PVC and its derivatives have been widely used in the lithography for preparation of integrated circuits and electronic components, as well as the micrographic processing of printed circuit boards, optical instruments, precision measuring tools and so on [**53**]. The preparation process of the PVC photoresist is simple, and only requires three chemical reagents (the PVC, an organic solvent and a sensitizing agent) that are inexpensive and commercially available. After being

patterned by UV irradiation and developing, a graphics with good resolution is often obtained (on a suitable substrate) for three reasons [**54**]: (i) the molecular weight distribution of PVC is relatively narrow, (ii) the photosensitive speed is uniform during exposure, and (iii) the molecular size is relatively even. In this paper, we report a PVC photoresist-based photolithographical patterning approach for fabrication of cloth-based microfluidic devices. It involves the use of photoresist and UV light to construct hydrophobic-hydrophilic structures on the cotton cloth. The hydrophobic photoresist is laboratory-formulated from low-cost, commercially available reagents. In addition, no clean-room or sophisticated facilities are required. Therefore, the proposed method for fabrication of μCADs is straightforward and inexpensive. This study was carried out in three parts. We first studied the wicking property of the cloth channel before and after fabrication of μCADs. Using a protocol similar to earlier works [**23, 55-58**], the pretreatment method using sodium hydroxide (NaOH) has been used to increase wicking or wetting properties of cotton cloth. In addition, the sodium dodecyl sulfate (SDS)-based post-treatment method has been proposed to increase the hydrophilicity of the cloth channels. Next, we studied the smallest dimensions for the width of hydrophobic barriers and hydrophilic channels. Finally, the high-throughput μCADs fabricated by photolithography were used for colorimetric assays of glucose and protein in artificial urine samples.

2. Experimental section

2.1. Materials and reagents

White plain weave cotton cloths (100% cotton, unmercerized, ~130 μm in thickness, having

65.59 denier, or 7.29 mg m^{-1} and a fabric count of 80 × 80, with 96 warp threads per inch and 88 weft threads per inch) were bought from Guangzhou Haiyin clothing wholesale Market (Guangzhou, China). Glucose oxidase, glucose and potassium chloride were purchased from Sigma-Aldrich (St. Louis, MO, USA). Urea, uric acid and creatinine were obtained from J & K scientific Ltd. (Beijing, China). Horseradish peroxidase, acetic acid, sodium chloride, sodium citrate dihydrate, ammonium chloride, calcium chloride dihydrate, magnesium sulfate heptahydrate, sodium bicarbonate, sodium sulfate anhydous, sodium oxalate, sodium dihydrogen phosphate monohydrate, sodium hydrogen phosphate, potassium iodide, trehalose dihydrate, anhydrous citric acid, anhydrous ethanol, bovine serum albumin (BSA) and bromophenol blue (BPB) were purchased from Sangon Biotech (Shanghai) Co., Ltd. (Shanghai, China). NaOH, butanone, and acetone were bought from Guangzhou Chemical Reagent factory (Guangzhou, China). Carmine food dye was obtained from Chengdu Xiya Chemical Technology Co., Ltd. (Chengdu, China). Cyclohexanone and 5-nitroacenaphthene were purchased from Chengdu Ai Keda Chemical Technology Co., Ltd. (Chengdu, China). PVC was bought from Shenzhen Shijingu Technology Co., Ltd. (Shenzhen, China). SDS was purchased from Tianjin Damao Chemical Reagent Factory (Tianjin, China). All solutions were prepared using deionized water (≥18 MΩ, ELGA PURELAB® Option-R15, London, UK) and stored at 4 ^{o}C in a refrigerator.

2.2. Instrumentation

A metal halide lamp (320-400 nm, 400 W, Philips HPA 400S) was chosen to polymerize photoresist in cloth. A Canon camera (Digital IXUS 60) was used for imaging and videoing.

A Canon scanner (Cano Scan LioE 110) was utilized for acquiring images of colorimetric detection of glucose or protein in μCADs, which were analyzed by Adobe Photoshop 7.0 and Origin 8.0 softwares. Photomasks for lithography were designed by Adobe Illustrator CS4 software and subsequently printed onto a transparency using a laser printer in Guangzhou Haochuang Computer Technology Co., Ltd. (Guangzhou, China). An oven (DHG-9035A, Shanghai Tensuc Experimental Instrument Manufacturing Co Ltd.) was used to dry various cloth-based samples during preparation of μCADs. A scanning electronic microscope (SEM) (ZEISS Ultra 55, Carl Zeiss, Germany) was used to analyze the features of the cloth fabrics in device fabrication. The energy dispersive spectrometer (EDS) (Oxford X-Max 50) analysis, which was attached to the ZEISS Ultra 55, was performed to confirm the surface chemical constitution in the cloth fabrics. A water-purification system (≥18 MΩ, ELGA PURELAB® Option-R15, London, UK) was used to obtain deionized water.

2.3. Pretreatment of the cloths used for microfluidic analytical devices

White plain weave cotton cloths served as the substrate material to fabricate μCADs. Before fabrication, cotton cloths were pretreated using NaOH, and the pretreatment process was somewhat different from that presented in previous reports [**23, 55-58**]. The cloth was first cut into size-predetermined pieces as samples for different pretreatments performed in this experiment. Then, these small pieces were put into NaOH solution (20 wt%) for 5-10 min at room temperature, followed by fully washing with water. After that, each piece of cloth was placed onto a square-shaped iron holder (outer edge size: 150 mm×150 mm; inner edge size: 130 mm×130 mm; thickness: 1 mm), and was tightened and smoothened by clips.

Subsequently, it was rinsed with sufficient amounts of SDS and water to remove the possible fat and smudginess. Next, to remove a small amount of NaOH residue, acetic acid solution (1 wt%) was sprayed onto the cloth fabric to neutralize the NaOH, followed by rinsing with plenty of water. Finally, the cloth samples were put into the oven for baking at 80 ^{o}C for 15 min before being used for testing.

2.4. Photolithographical fabrication for μCADs

We defined and created hydrophilic/hydrophobic regions on the pretreated cloth fabric by photolithography. To reduce the cost of fabrication, a negative PVC photoresist which contained PVC (15.0 wt%), cyclohexanone (84.7 wt%) and 5-nitroacenaphthene (0.3 wt%), was produced in-house from commercially available reagents. The production process of PVC photoresist could be described as follows: we firstly took 150 mL of cyclohexanone in a beaker. Then, 25.236 g of PVC and 0.5047 g of 5-nitroacenaphthene were weighed and sequentially put into the cyclohexanone-containing beaker, followed by stirring in the dark for 20 min to dissolve them well. Finally, the mixed solution was transferred into a brown bottle which should be stored in a dark place. The obtained mixture (i.e. PVC photoresist) could be used for fabricating of a number of μCADs. The fabricating process of μCADs is shown in **Figure 1** and described as follows: Firstly, 2.5 mL of PVC photoresist was coated onto the pretreated cloth substrate (130 mm×130 mm) on square-shaped iron holder by using a hard, smooth poly(ethylene terephthalate) (PET) slice. Secondly, the cloth fabric together with the iron holder was put into the oven and baked at 80 ^{o}C for 20 min to remove the solvent (cyclohexanone) in the PVC photoresist. Thirdly, the cloth fabric was separated from

the iron holder after prebaking was completed, and then exposed to UV light for 3 min through the photomask which was pressed with a quartz glass. During the exposure, the back of the cloth sheet was protected from UV light. After exposure, the quartz glass and photomask were removed, and then the exposed cloth fabric was baked for a second time in the oven at 95 ^{o}C for 2 min to cross-link the exposed portions of the photoresist. After post-baking, the cloth fabric was soaked and shaken in a PVC developer (butanone) for 3 min, then in acetone for 1 min to remove the unpolymerized photoresist, resulting in the formation of the hydrophobic patterns on the cloth. To further remove the possible residues of photoresist in hydrophilic patterns, the cloth-based device was rinsed with plenty of water. In addition, to increase the hydrophilicity of the cloth-based channels, the μCAD was washed with SDS or NaOH solution (3 wt%) for 5 min. Finally, the patterned cloths were rinsed with water and then dried in the oven at 65 ^{o}C for 15 min.

2.5. Biochemical assays on μCADs

To demonstrate applications of μCADs fabricated by photolithography, the colorimetric assays of glucose and BSA were carried out in artificial urine samples. For the glucose assay, the same detection reservoirs (ø 3.5 mm) in a μCAD were employed as the sampling zones. Here, each detection reservoir was preloaded with a solution (0.7 μL) containing 0.6 M potassium iodide, 0.3 M trehalose and glucose oxidase-horseradish peroxidase (120 units of glucose oxidase enzyme activity and 30 purpurogallin units of horseradish peroxidase enzyme activity per mL of solution). The cloth device was allowed to dry at room temperature for 10 min. For the protein assay, the detection reservoir (ø 3 mm) was connected

with a sampling zone (ø 5 mm) by a 5 mm × 1 mm hydrophilic channel. And, we spotted into the detection zone 0.7 μL of a 250-mM citrate buffer solution (pH 1.8), followed by 10 min of drying, and then 0.2 μL of a 9-mM BPB solution in 95% (v/v) of ethanol with 5% (v/v) of water, followed by 5 min of drying. The prespotted devices were stored at room temperature in a closed environment. When biomedical assays were performed, the artificial urine samples containing glucose or BSA were spotted into the sampling zone.

2.6. Data acquisition and analysis

2.6.1. Testing of the wicking property of the cloth

The dumbbell-shaped test region in a cloth-based device was designed for simple testing of the wicking property of the cloth fabrics (**Figure S1**, the inlet and outlet zones (ø 8 mm each) are connected by a 20 mm×2 mm channel). The wicking property of different cloth samples (such as cloth pieces prepared by a cutter and μCADs fabricated by photolithography) was assessed by recording the wicking time via a camera, during which 12- or 16-μL carmine dye solution flowed horizontally from the inlet to the outlet through a 20-mm channel. And, the shorter the time requires, the faster the wicking of sample. As a result, the cloth fabric is more hydrophilic.

2.6.2. Assays of glucose or BSA in artificial urine

A certain amount of glucose or BSA was added to artificial urine to simulate a body analyte. The artificial urine was prepared according to the protocol proposed in previous reports [**23, 59**]. The artificial urine contains 202 mM urea, 1 mM uric acid, 4 mM creatinine, 5 mM

sodium citrate, 54 mM sodium chloride, 30 mM potassium chloride, 15 mM ammonium chloride, 3 mM calcium chloride, 2 mM magnesium sulfate, 2 mM sodium bicarbonate, 0.1 mM sodium oxalate, 9 mM sodium sulfate, 3.6 mM sodium dihydrogen phosphate and 0.4 mM sodium hydrogen phosphate, all mixed in 200 mL of deionized water. For the glucose assay, 1.0 μL of artificial urine was dropped into the detection reservoir, and allowed to react with the preloaded reagents for about 20 min. During the reaction, the brown colors of the detection reservoir were gradually changed from shallow to deep brown. For the BSA assay, a droplet of artificial urine (2.5 μL) was added into the inlet, and then moved into the detection reservoir by capillary action. And, the detection reservoirs gave cyan colors after tens of seconds, but another time interval of about 10 min was required for the color to fully develop. To quantify the color of the glucose assay zone, the flatbed scanner was used to acquire the image of cloth-based device at 600 dpi, which was imported into Adobe Photoshop 7.0 and then transferred to 8-bit grayscale mode. Next, the region of detection reservoir in the image was selected by a marquee tool, and its mean gray value was generated from the image histogram. And, this gray value was background-corrected by subtracting the measured average detection zone intensity from the mean intensity of the blank control where no glucose was added to the reaction mixture. Based on these corrected mean gray values, the calibration curve was generated in Origin 8.0 software. When the BSA assays were performed, a similar procedure was utilized except that the CMYK mode and cyan channel was applied for quantifying the colorimetric responses.

3. Results and discussion

3.1. Choice of PVC photoresist and the photostimulation-induced cross-linking mechanism

The PVC photoresist was chosen to fabricate the μCADs for the following reasons: (i) Its components are easily available commercially, and it can be conveniently self-made in an ordinary laboratory. (ii) Its cost is much less than that of the SU-8 photoresist which has been commonly used in conventional micro-electro-mechanical-systems (MEMS) and microfluidic fields. The laboratory-formulated PVC photoresist costs ~\$30 L^{-1}, while the commercial, small-volume price of SU-8 is approximately \$800 L^{-1} [**25**]. (iii) Its resolution is high (i.e., the resulting photolithography has small line edge's transition zone, clear graphics and steep edges) [**54**], and thus the hydrophobic-hydrophilic boundary on cloth can be well formed. (iv) It has some other characteristics such as high sensitivity, high stability, strong resistance to corrosion, strong adhesion, high cleanliness and good resistance to moisture [**54**]. For the PVC photoresist, its photostimulation-induced cross-linking mechanism can be simply described as follows [**60, 61**]: the carbon-carbon double bond of cinnamoyl groups in the PVC resist system undergoes a photodimerization reaction upon irradiation with UV light (**Figure S2**). This dimerization reaction results in the intermolecular cross-linking of PVC and thus becomes a kind of polymer which shows infinite differential solubility between exposed and unexposed polymer for the used PVC developer solution (butanone). It should be noted that in the present PVC system, 5-nitroacenaphthene, which is usually applied in negative photoresists [**62**], is used as a sensitizer to enhance the sensitivity of PVC.

3.2. Evaluation of wicking property of the cloth in the fabrication process

3.2.1. NaOH pretreatment for improving wicking in cloth

The "wicking" is termed as a spontaneous transport of a liquid driven into a porous system (such as cloth, thread or paper) by capillary forces. Generally, the non-cellulosic components of cotton fiber surface (for example cuticle, wax, protein and fats) have adverse effects on the wicking of cotton fiber [**23, 55-58**]. To improve the wicking property in cloth, therefore, the cloth fabric was pretreated by immersing it in 20 wt% NaOH solution for a certain period of time (0 min, 5 min, and 10 min). And, two different volumes of carmine dye solution (12 μL and 16 μL) were added onto the inlet of test zone to study the wicking rate in cloth. As shown in the left three columns of **Figure 2(A)**, the dye solution spent less time on flowing through the cloth piece pretreated for 5 or 10 min, implying that the wicking rate in the pretreated cloth fabrics was increased. To understand the possible reasons of this phenomenon, three cloth pieces pretreated for different time lengths were first analyzed by SEM. As we can see from the SEM images (100×) in **Figure S3** and the SEM images (500×) in **Figure 2(B)(i, ii)** and **Figure S4**, the yarns in the pretreated cloth pieces got closer than those without any treatment. This may result from the fact that the cloth pretreatment using NaOH solution of high concentrations causes the longitudinal shrinkage and lateral swelling of cotton fibers in a single yarn [**63-65**]. In addition, possibly because the cuticle and hydrophobic wax layer of cotton fiber were partly removed [**23, 55-58**], the pretreated fiber surface became rougher and certain nanoscale gaps were formed on it (**Figure S5**), and the underlying cellulose fibrous structure being rich in hydrophilic hydroxyl groups was exposed. To further investigate the surface of cotton fiber, the EDS analysis of the pretreated cloth pieces was performed (**Table S1** and **Figure S6-8)**. As seen from **Table S1**, the cotton fibers pretreated for 5 or 10 min with

NaOH solution have an increase of approximately 1.91% or 1.75% in the oxygen to carbon atomicity ratio (O/C), as compared with those without any pretreatment. Generally, the increasing apparent oxygen at the surface makes the fiber surface more hydrophilic, thus improving its wettability to aqueous solutions [**23**]. According to the above-mentioned SEM and EDS results, it may be reasonable that the increased wicking in the pretreated cloth samples is due to the changes in chemical composition, physical structure and texture/morphology of the cotton fiber surface. The former two factors have increased the wettability, which is a prerequisite for the increased wicking. For the latter factors, the morphological surface roughness of NaOH-pretreated cotton fibers is increased. As a result, the surface to volume ratio is increased and the pressure gradient is added because of the occurrence of nanoscale capillary channels along the fiber, which contributes to the increased wicking rate in the pretreated cotton fabrics.

3.2.2. μCAD's photolithographical fabrication and its resulting decreased wicking

To demonstrate the effect of the presented patterning method on the wicking of the cotton fabric, the unpretreated and NaOH-pretreated cotton fabrics were used as the substrate material to photolithographically fabricate μCADs, and then the wicking rate (or wicking time) of dye solution in the μCAD's test channel was evaluated. According to the results in the fourth to sixth columns of **Figure 2(A)** (from left to right), several findings can be obtained as follows: (1) The patterned channel from the NaOH-pretreated cloth fabric maintained a faster wicking rate than the unpretreated one, as is similar to the case in the left three columns of **Figure 2(A)**. (2) The time the dye solution spent on flowing through the

NaOH-pretreated channel was about one-third of that through the unpretreated channel, as is not the same as that shown in the left three columns of **Figure 2(A)**. (3) The wicking time required in photolithographically patterned cloth channels was much longer than that observed in corresponding cloth pieces prepared by a cutter. These results indicate that the photolithographic patterning method can give rise to decreased wicking in cloth, although the NaOH-pretreatment makes the cotton fabric more hydrophilic and increases its liquid wicking property. To investigate the reasons for the decline in this wicking ability, SEM analysis was first used to obtain the images of test zone in μCADs fabricated with NaOH-pretreated cloth fabrics (**Figure 2(B)(iii)** and **Figure S19**). As shown in these SEM images, the residues of hydrophobic PVC photoresist clearly exist in the patterned hydrophilic region. Furthermore, the NaOH-pretreated μCADs seem to have less photoresist residues than the unpretreated ones, thus showing a relatively high hydrophilicity (or good wettability) (the fourth to sixth columns of **Figure 2(A)**). In fact, the EDS spectra also can prove this. The photolithographic patterning causes a decrease of 9.8%-13.4% in the O/C ratio of the fabrics surface, as listed in **Table S1** and shown in **Figure S9-11**. In the controlled cloth pieces which were not coated with photoresist but participated in the other procedures of lithography, however, almost no change in the O/C ratio was observed (**Table S1** and **Figure S18**). It is noteworthy that compared with the NaOH-pretreated μCAD's test zone, 0-min pretreated ones had a higher O/C ratio, but had lower hydrophilicity (**Table S1** and **Figure S9-11**). At present, we may have been unable to accurately pinpoint the source of this phenomenon, but we suspect that that one reason is that for a fabric made up of spun yarns, NaOH pretreatment can cause the shrinkage in warp and weft directions [**65**], as is similar to

the explanation related to the left three columns of **Figure 2(A)**.

3.2.3. Post-treatment of μCADs for increasing the hydrophilicity

It has been shown in previous reports [**2**, **31**, **32**, **43**, **45**, **48**] that the paper is more hydrophobic after it is photolithographically patterned, presumably owing to residual resist bound to the paper, and that the oxygen-plasma post-treatment technique can be employed to increase the hydrophilicity of the paper channels. Such post-treatment method usually requires a costly instrument the majority of labs may not afford. To circumvent this shortcoming, an inexpensive, NaOH or SDS-based post-treatment approach is developed, and it requires minimal external instrumentation for implementation in almost all of the labs. The right two columns of **Figure 2(A)** shows the assessment of wicking time of dye solution in 5-min NaOH-pretreated μCADs post-treated for 5 min with 3 wt% NaOH or SDS solution. As seen from the right two columns of **Figure 2(A)**, the wicking rate of NaOH or SDS-treated μCADs nearly returned to the original level in the left three columns of **Figure 2(A)**, implying that both chemical post-treatments can increase the hydrophilicity of the μCADs. Such phenomenon may be verified by the SEM results. As shown in **Figure 2(B)(iii, iv)** and **Figure S20**, the photoresist residues in the hydrophilic working zone could be partly removed after post-treatment using NaOH or SDS solution. However, surprisingly, less residues of photoresist remained on the SDS-post-treated working zone compared with those on the NaOH-post-treated working zone, even though similar wicking property was observed on these two working zones. As seen from the SEM results, NaOH or SDS-based post-treatment did not obviously cause the longitudinal shrinkage and lateral swelling of

cotton fibers. Therefore, it is logical and reasonable to suspect that other factors also affect the imbibition characteristics of the post-treated μCADs. Here, the elemental analysis of EDS spectra for two different specimens was designed to further evaluate this phenomenon. As shown in **Table S1** and **Figure S12, 13**, the O/C radios on the working zones post-treated with SDS and NaOH were increased by 5.9% and 1.8%, respectively, relative to the result stated in **Figure S10**. However, these two O/C radios were lower compared with those in the controlled cloth pieces (**Table S1 and Figure S16, 17**). These changes in the O/C ratio seem to well correspond to the SEM results. In addition, it should be noted that after chemical post-treatment the μCAD's hydrophobic zone still had a much lower O/C radio (**Figure S14, 15**) and a large number of hydrophobic photoresist materials (**Figure S21**). Importantly, the boundary between hydrophilic and hydrophobic areas in μCADs was clearly observed (**Figure S22**), and even the gaps between the single cotton fibers in the hydrophilic zone (**Figure S23**) were obviously different from those in the hydrophobic zone (**Figure S21(B, D)**). It can be inferred therefore that the developed post-treatment method does not destroy the formation of hydrophobic barrier for defining microfluidic zones in cloth. Finally, it needs to be demonstrated that both post-treatments are quick, simple, and inexpensive methods for promoting hydrophilicities of the μCADs, but that the SDS-based post-treatment may be more effective than the NaOH-based one, as seen from the right two columns of **Figure 2(A)**. Therefore, the SDS-based post-treatment approach was chosen to increase the hydrophilicity of the cloth-based devices in later experiments.

3.3. Resolution of the photolithographical patterning method for μCADs

In previously reported μCAD's fabricating methods such as weaving [**20**-**22**] and wax patterning [**23**], there have been no studies on resolution of the relevant fabrication methods. In the present work, we try to determine the resolution of structures fabricated in cloth using photolithography, because the resolution of patterning method determines to some extent to the application fields of patterned μCADs as well as integration, miniaturization and throughput levels of chip's device. To define the resolution of the photolithographical patterning method, we evaluated experimentally the channel width of the narrowest functional hydrophilic channel and the barrier width of the narrowest functional hydrophobic barrier. A functional hydrophilic channel can be defined as one that is at least 5-mm long and wicks dye solutions from a fluid reservoir to a test zone, and a functional hydrophobic barrier is defined as one that prevents dye solutions from wicking across it for at least 30 min.

3.3.1. Resolution of the hydrophilic patterns

To study the relationship between the actual widths of the hydrophilic channel and the initial channel widths on the photomask, a series of straight channels that were defined as the nominal space of two parallel hydrophobic barriers and that were connected to two circles (the big one as a fluid reservoir and the small one as a test zone), were designed on a photomask, whose sizes in width varied from 100 to 1000 μm in increments of 100 μm (**Figure 3(A)**). **Figure 3(B)** shows the resulting hydrophilic channels after adding dye solutions into the fluid reservoirs on the μCAD. It can be seen from **Figure 3(B)** that the narrowest designed channel in which the dye solution could pass was 500 μm, which can be deemed as the highest resolution of the hydrophilic channel the photolithographical patterning method can achieve in the cotton cloth. And, a plot of the resulting channel widths

versus the designed width from the photomask is shown in **Figure 3(C)**. It has been demonstrated in this plot that in the range of 600-1000 μm the measured value of the channel width was about 250 μm larger than the corresponding designed one, and that in the case of 500 μm the difference between two channel widths was up to 315 μm. To a surprising extent this variability is greatly different from that observed in photolithographically patterned papers in a previous report [**44**]. In these chromatography paper-based devices, the smallest functional hydrophilic channel was designed to be 250 μm in width and was measured to be 256±20 μm. We suspect that the variance in resolution of the hydrophilic channel is most likely due to the difference in thickness of the substrate, especially in structure of the substrate itself. Different from paper, the cloth used here is composed of woven threads in warp and weft directions, which are perpendicular to each other. It is a hierarchical structure made from spun fibers and woven threads [**66**]. In our case presented in this paper, the cotton cloth is wettable by fluids through interstitial spaces not only between the fibers in a single thread but also between its woven threads [**23**].

3.3.2. Resolution of the hydrophobic patterns

A series of square-shaped hydrophobic barriers with widths varying from 100 to 600 μm in steps of 100 μm, were structured to characterize the smallest photoresist line width to confine the liquid, which separated a centre hydrophilic zone (as a fluid reservoir or a test zone) from a concentric annular hydrophilic zone (**Figure 4(A)**). **Figure 4(B)** shows a representative μCAD with a series of hydrophilic-hydrophobic patterns, while **Figure 4(C, D)** demonstrates the images of representative μCADs where food dye solution was added into the centre or

concentric annular hydrophilic zone. It can be clearly seen from **Figures 4(C, D)** and **S24** that even the 100 μm designed line of photoresist can still function well as the hydrophobic barrier after photolithographical patterning because only 2 out of 21 100-μm-wide hydrophobic barriers in three different μCADs are penetrated through by the dye solution. Perhaps even more meaningful is that the obtained resolution for hydrophobic barrier is comparable to what Martinez et al. reported in a paper-based device where the smallest functional SU-8 barrier was designed to be 200 μm in width [**44**]. In addition, this minimum functional barrier width is much smaller than that shown in a previous report where the smallest barrier width for paper-based devices was 250 μm in designed width [**38**]. In the present work, the factors contributing to the increased resolution of the hydrophobic patterns are difficult to be precisely evaluated. But, one of the possible reasons for this is the use of thin cloth substrate and thin PVC photoresist.

3.4. Colorimetric assays in μCADs

In this study, colorimetric detection of glucose and protein was used as a model assay to evaluate the function of μCADs as an analytical device. In order to make this evaluation more representative, two different types of arrayed, high-throughput cloth-based microfluidic devices were designed and fabricated. On one arrayed device (Design 1), the same fluid reservoir of the μCAD was employed as the test zone. For another arrayed device (Design 2), the test zone of μCAD was connected with a fluid reservoir via a hydrophilic channel. By the way, these two kinds of designs of array pattern are commonly used for applications of paper-based microfluidic devices, but so far they have not been applied for bioassays in

μCADs.

Firstly, colorimetric bioassays of glucose in artificial urine samples were performed in μCADs with Design 1. As shown in **Figure 5(A)**, the colour intensity was allowed to develop from shallow brown to a strong brown within about 20 min, which corresponded well to the concentration range of glucose in artificial urine (0-20 mM). The test zone in **Figure 5(A)** has a designed diameter of 3.5 mm and it is defined to be small enough to decrease the sample consumption volume (only 1 μL), but the assay results are still observable by naked eye. It should be noted that Wicaksono and co-workers have recently developed cloth-based ELISA microzones with two rows and six columns of circles to detect human chorionic gonadotropin [**24**]. In their work, the volume required for the similar cloth microzones (ø 3.5 mm) was optimized to be 3 μL. **Figure 5(B)** shows a calibration curve for glucose concentration versus colour intensity. Overall, the present glucose assay showed an acceptable linear range between 0 to 20 mM (n = 6, $R^2 = 0.9793$), and the limit of detection (LOD) based on three times standard deviation of the blank response was calculated to be 0.74 mM. These results are comparable to those reported in a previous paper-based device [**38**] where the glucose assay in the linear range of 3-50 mM had the LOD of 2.8 mM and 5 μL of the sample was required to spot on the sample pad. Here, it is worth pointing out that it is for the first time that our μCADs are used for glucose diagnostic applications, but that the assays in μCADs still need to be optimized to improve the LOD as well as the linear range.

Next, the μCADs with Design 2 were fabricated for colorimetric assay of protein in artificial urine samples. Here, 2.5 μL of the sample was spotted onto the fluid reservoir and allowed to wick down a channel and into the test zone where it came into contact with the

detection reagents. The sample filled the entire pattern within about 2 min, but the assays required approximately 10 min for the cloth to dry and for the color to fully develop. In all cases, color changes were observed, corresponding roughly in intensity to the amount of BSA in the test samples (**Figure 5(C, D)**). As shown in **Figure 5(D)**, the color intensity changed almost linearly with the BSA concentration between 0 and 50 mM with an estimated LOD of 8.09 mM ($n = 6$, $R^2 = 0.9784$). This result indicates that the photolithographically patterned μCADs have the potential for quantitative detection of protein in urine samples. It has been shown in a previous report that the μCADs fabricated using a wax patterning technique could also be applied for colorimetric protein assay in artificial urine [**23**]. In their work, however, no quantitative or high-throughput assays have been reported.

4. Conclusions

This paper demonstrates that microfluidic analytical devices can be fabricated by photolithography using cotton cloth as the structural material. For the presented fabrication method, the PVC photoresist is laboratory-formulated from commercially available reagents and it is much more inexpensive than the widely used SU-8 photoresist. And, the cheap cotton cloth is utilized in this method as substrate material. In addition, simple and low-cost chemical pre- or post-treatment approaches have been employed to promote hydrophilicity in μCADs. As a result, the whole fabrication of μCADs is low-cost, straight-forward and can be carried out in any laboratory without specialized equipment and clean room facility.

The present method described for fabricating μCADs are high in resolution. The resolution for hydrophilic channels is designed to be 500 μm and that for

between-hydrophilic zone hydrophobic barrier is designed to be 100 μm. Such a resolution may be appropriate for performing high-throughput cloth-based bioassays where a very small amount of samples and reagents are used in each unit. As a conceptual description, the colorimetric assays for glucose and protein in artificial urine samples have been performed on two different high-throughput μCADs, and the colorimetric results can be designed to be observable by direct visual observation for quick diagnosis. It can be foreseen, therefore, that photolithographically patterned μCADs will open new possibilities and bring broad applications in clinical diagnosis, food safety detection and environmental monitoring.

Acknowledgements

This research is supported by the National Natural Science Foundation of China (61072030) and the project of Guangzhou science and technology plan 2014 (2014J4100030).

References

1. P. Yager, G. J. Domingo and J. Gerdes, *Annu. Rev. Biomed. Eng.*, 2008, **10**, 107-144.
2. A. W. Martinez, S. T. Phillips, M. J. Butte and G. M. Whitesides, *Angew. Chem. Int. Ed.*, 2007, **46(8)**, 1318-1320.
3. A. W. Martinez, S. T. Phillips and G. M. Whitesides, *Anal. Chem.*, 2010, **82(1)**, 3-10.
4. A. K. Yetisen, M. S. Akram and C. R. Lowe, *Lab Chip*, 2013, **13(12)**, 2210-2251.
5. A. Nilghaz, D. R. Ballerini and W. Shen, *Biomicrofluidics*, 2013, **7(5)**, 051501.
6. D. R. Ballerini, X. Li and W. Shen, *Anal. Bioanal. Chem.*, 2011, **399(5)**, 1869-1875.
7. D. R. Ballerini, X. Li and W. Shen, *Biomicrofluidics*, 2011, **5**, 014105.

8. D. R. Ballerini, Y. H. Ngo, G. Garnier, B. P. Ladewig, W. Shen and P. Jarujamrus, *AIChE J.*, 2014, **60(5)**, 1598-1605.

9. S. S. Banerjee, A. Roychowdhury, N. Taneja, R. Janrao, J. Khandare and D. Paul, *Sens. Actuators B*, 2013, **186**, 439-445.

10. V. F. Curto, S. Coyle, R. Byrne, N. Angelov, D. Diamond and F. Benito-Lopez, *Sens. Actuators B*, 2012, **175**, 263-270.

11. W. I. S. Galpothdeniya, K. S. McCarter, S. L. De Rooy, B. P. Regmi, S. Das, F. Hasan, A. Tagge and I. M. Warner,. *RSC Adv.*, 2014, **4(14)**, 7225-7234.

12. T. Guinovart, M. Parrilla, G. A. Crespo, F. X. Rius and F.J. Andrade, *Analyst*, 2013, **138(18)**, 5208-5215.

13. X. Li, J. F. Tian and W. Shen, *ACS Appl. Mater. Interfaces*, 2010, **2(1)**, 1-6.

14. A. Nilghaz, D. R. Ballerini, X. Y. Fang and W. Shen, *Sens. Actuators B*, 2014, **191**, 586-594.

15. M. Reches, K. A. Mirica, R. Dasgupta, M. D. Dickey, M. J. Butte and G. M. Whitesides, *ACS Appl. Mater. Interfaces*, 2010, **2(6)**, 1722-1728.

16. R. Safavieh, G. Z. Zhou and D. Juncker, *Lab Chip*, 2011, **11(15)**, 2618-2624.

17. S. Y. Xing, J. Jiang and T. R. Pan, *Lab Chip*, 2013, **13(10)**, 1937-1947.

18. Y. A. Yang, C. H. Lin and Y. C. Wei, *Microfluid. Nanofluid.*, 2014, **16(5)**, 887-894.

19. G. Zhou, X. Mao and D. Juncker, *Anal. Chem.*, 2012, **84(18)**, 7736-7743.

20. P. Bhandari, T. Narahari and D. Dendukuri, *Lab Chip*, 2011, **11(15)**, 2493-2499.

21. T. L. Owens, J. Leisen, H. W. Beckham and V. Breedveld, *ACS Appl. Mater. Interfaces*, 2011, **3(10)**, 3796-3803.

22. F. Vatansever, R. Burtovyy, B. Zdyrko, K. Ramaratnam, T. Andrukh, S. Minko, J. R. Owens, K. G. Kornev and I. Luzinov, *ACS Appl. Mater. Interfaces*, 2012, **4(9)**, 4541-4548.

23. A. Nilghaz, D. H. B. Wicaksono, D. Gustiono, F. A. Abdul Majid, E. Supriyanto and M. R. Abdul Kadira, *Lab Chip*, 2012, **12(1)**, 209-218.

24. S. Bagherbaigi, E. P. Córcoles and D. H. B. Wicaksono, *Anal. Methods*, 2014, **6(18)**, 7175-7180.

25. R. S. P. Malon, K. Y. Chua, D. H. B. Wicaksono and E. P. Córcoles, *Analyst*, 2014, **139(12)**, 3009-3016.

26. A. Apilux, W. Dungchai, W. Siangproh, N. Praphairaksit, C. S. Henry and O. Chailapakul, *Anal. Chem.*, 2010, **82**, 1727-1732.

27. E. Carrilho, S. T. Phillips, S. J. Vella, A. W. Martinez and G. M. Whitesides, *Anal. Chem.*, 2009, **81**, 5990-5998.

28. H. Chen, J. Cogswell, C. Anagnostopoulos and M. Faghri, *Lab Chip*, 2012, **12**, 2909-2913.

29. X. Chen, J. Chen, F. B. Wang, X. Xiang, M. Luo, X. H. Ji and Z. K. He, *Biosens. Bioelectron.*, 2012, **35**, 363-368.

30. C. M. Cheng, A. W. Martinez, J. L. Gong, C. R. Mace, S. T. Phillips, E. Carrilho, K. A. Mirica and G. M. Whitesides, *Angew. Chem. Int. Ed.*, 2010, **49**, 4771-4774.

31. W. Dungchai, O. Chailapakul and C. S. Henry, *Anal. Chem.*, 2009, **81**, 5821-5826.

32. W. Dungchaia, O. Chailapakul and C. S. Henry, *Anal. Chim. Acta*, 2010, **674**, 227-233.

33. A. K. Ellerbee, S. T. Phillips, A. C. Siegel, K. A. Mirica, A. W. Martinez, P. Striehl, N.

Jain, M. Prentiss and G. M. Whitesides, *Anal. Chem.*, 2009, **81**, 8447-8452.

34. W. L. Gu, Y. H. Xu, B. H. Lou, Z. Z. Lyu and E. K. Wang, *Electrochem. Commun.*, 2014, **38**, 57-60.
35. P. D. Haller, C. A. Flowers and M. Gupta, *Soft Matter*, 2011, **7**, 2428-2432.
36. Q. H. He, C. C. Ma, X. Q. Hu and H. W. Chen, *Anal. Chem.*, 2013, **85**, 1327-1331.
37. H. Kim and H. Noh, *Macromol. Res.*, 2013, **21(7)**, 788-792.
38. S. A. Klasner, A. K. Price, K. W. Hoeman, R. S. Wilson, K. J. Bell and C. T. Culbertson, *Anal. Bioanal. Chem.*, 2010, **397**, 1821-1829.
39. H. Liu and R. M. Crooks, *J. Am. Chem. Soc.*, 2011, **133**, 17564-17566.
40. B. H. Lou, C. G. Chen, Z. X. Zhou, L. L. Zhang, E. K. Wang and S. J. Dong, *Talanta*, 2013, **105**, 40-45.
41. C. C. Ma, Z. Q. Bai, Q. H. He and H. W. Chen, 16th International Conference on Miniaturized Systems for Chemistry and Life Sciences; October 28 - November 1, 2012; Okinawa, Japan; pp. 1261-1263.
42. A. W. Martinez, S. T. Phillips, E. Carrilho, S. W. Thomas III, H. Sindi and G. M. Whitesides, *Anal. Chem.*, 2008, **80(10)**, 3699-3707.
43. A. W. Martinez, S. T. Phillips and G. M. Whitesides, *Proc. Natl. Acad. Sci. USA*, 2008, **105**, 19606-19611.
44. A. W. Martinez, S. T. Phillips, B. J. Wiley, M. Gupta and G. M. Whitesides, *Lab Chip*, 2008, **8**, 2146-2150.
45. A. W. Martinez, S. T. Phillips and G. M. Whitesides, *Lab Chip*, 2010, **10**, 2499-2504.
46. Z. Nie, C. A. Nijhuis, J. Gong, X. Chen, A. Kumachev, A. W. Martinez, M.

Narovlyansky and G. M. Whitesides, *Lab Chip*, 2010, **10**, 477-483.

47. D. Pardasani, V. Tak, A. K. Purohit and D. K. Dubey, *Analyst*, 2012, **137**, 5648-5653.
48. P. Rattanarat, W. Dungchai, W. Siangproh, O. Chailapakul and C. S. Henry, *Anal. Chim. Acta*, 2012, **744**, 1-7.
49. A. R. Rezk, A. Qi, J. R. Friend, W. H. Li and L. Y. Yeo, *Lab Chip*, 2012, **12**, 773-779.
50. Y. H. Xu, B. H. Lou, Z. Z. Lv, Z. X. Zhou, L. B. Zhang and E. K. Wang, *Anal. Chim. Acta*, 2013, **763**, 20-27.
51. Y. H. Xu, Z. Z. Lv, Y. Xia, Y. C. Han, B. H. Lou and E. K. Wang, *Anal. Bioanal. Chem.*, 2013, **405(11)**, 3549-3558.
52. US Pat., 2 690 966, 1954.
53. J. H. Zheng, *Fine Specialty Chem.*, 2006, **14(16)**, 24-30.
54. Y. Shao, J. S. Jiang and C. R. Xu, *Shanghai Chem. Ind.*, 1999, **24(3, 4)**, 36-37.
55. J. J. de Boer, *Text. Res. J.*, 1980, **50(10)**, 624-631.
56. Y. L. Hsieh, J. Thompson and A. Miller, *Text. Res. J.*, 1996, **66(7)**, 456-464.
57. R. Mitchell, C. M. Carr, M. Parfitt, J. C. Vickerman and C. Jones, *Cellulose*, 2005, **12**, 629-639.
58. I. Jordanov and B. Mangovska, *Open Text. J.*, 2009, 2, 39-47.
59. S. Chutipongtanate and V. Thongboonkerd, *Anal. Biochem.*, 2010, **402**, 110-112.
60. S. Nanjundan and C. S. J. Selvamalar, *J. Macromol. Sci. Part A-Pure Appl. Chem.*, 2006, **43(8)**, 1189-1203.
61. U. Okoroanyanwu, in Chemistry and Lithography, SPIE Press, 2010, ch. 6, pp. 203-204.
62. J. P. Han, H. L. Zhong, J. R. Ma and S. W. Wang, *Acta Electron. Sini.*, 1985, **13(3)**,

36-41.

63. A. R. Moghassem and M. R. Bakhshi, *Fiber. Polym.*, 2009, **10(6)**, 847-854.

64. A. R. Moghassem and P. Valipour, *Fiber. Polym.*, 2013, **14(2)**, 330-337.

65. N. Sameii, S. M. Mortazavi, A. S. Rashidi and S. Sheikhzadah-Najar, *J. Applied Sci.*, 2008, **8(22)**, 4204-4209.

66. S. V. Lomov, G. Huysmans and I. Verpoest, *Text. Res. J.*, 2001, 7**1(6)**, 534-543.

Figure Captions

Figure 1. Schematic of the photolithographical fabrication procedure of microfluidic cloth-based analytical devices (μCADs).

Figure 2. **(A)** Effect of different pre- or post-treatments on the wicking property of cloth samples (cloth pieces or μCADs). (**B**) SEM images (500×) showing the hydrophilic part of non-treated cloth piece (**i**), 5-min NaOH pretreated cloth piece before photolithography (**ii**), μCADs with 5-min NaOH pretreatment and no post-treatment (**iii**), or μCADs with 5-min NaOH pretreatment and 5-min SDS post-treatment (**iv**). In (**A**), the error bar is the standard deviation from six independent experiments.

Figure 3. Resolution of the photolithographically patterned hydrophilic channels. (**A**) Designed widths of functional hydrophilic cloth channels ranging from 100 μm to 1000 μm; (**B**) Images of the photolithographically patterned hydrophilic channels dotted with carmine food dye solution. The solution flowed through the test channel from the big circle to the small circle; (**C**) Illustration of resulting channel widths relative to designed channel widths. In (**C**), the error bar is the standard deviation from fifteen independent experiments.

Figure 4. Resolution of the photolithographically patterned hydrophobic barrier widths. (**A**) Design of functional hydrophobic barriers. A series of hydrophobic square-shaped barriers were constructed, with nominal widths of inner barriers ranging from 100 μm to 600 μm and nominal widths of outer barriers being 300 μm; (**B**) Image of a representative μCAD with a series of hydrophilic-hydrophobic patterns. Here, it needs to note that the color, brightness, contrast and saturation of original μCAD image obtained by the scanner has been properly adjusted by Adobe Photoshop 7.0 software so as to clearly discern the

hydrophilic-hydrophobic boundaries; (**C**, **D**) Images of the μCADs whose inner or outer hydrophilic zones were filled with food dye solution.

Figure 5. Application of μCADs for glucose and protein colorimetric assays. (**A**, **B**) The photograph and quantitative calibration curve of colorimetric detection of glucose. Here, the detection reservoirs on a μCAD were employed as the sampling zones, and the concentrations of glucose in artificial urine were 0 mM, 2.5 mM, 5 mM, 10 mM, and 20 mM, respectively; (**C**, **D**) The photograph and quantitative calibration curve of colorimetric detection of BSA. On each μCAD, the working zone was connected with a sampling inlet. And, the BSA concentrations in artificial urine were 0 μM, 10 μM, 20 μM, 35 μM, and 50 μM, respectively. In (B) and (D), the error bar is the standard deviation from six independent experiments.

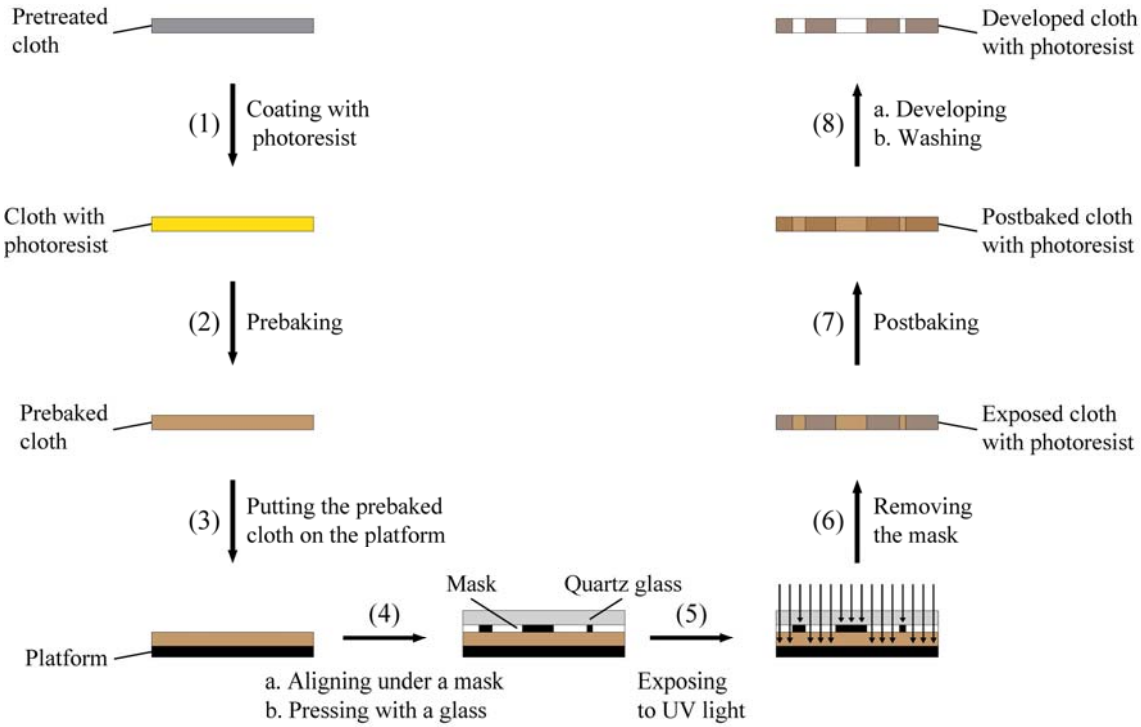

Figure 1

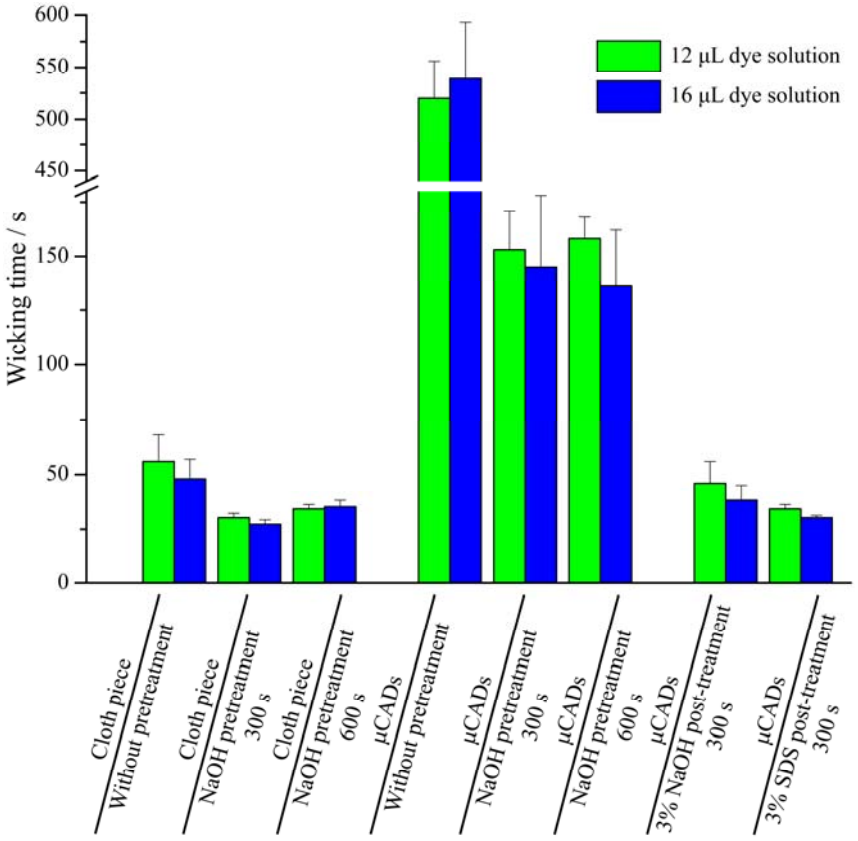

(A)

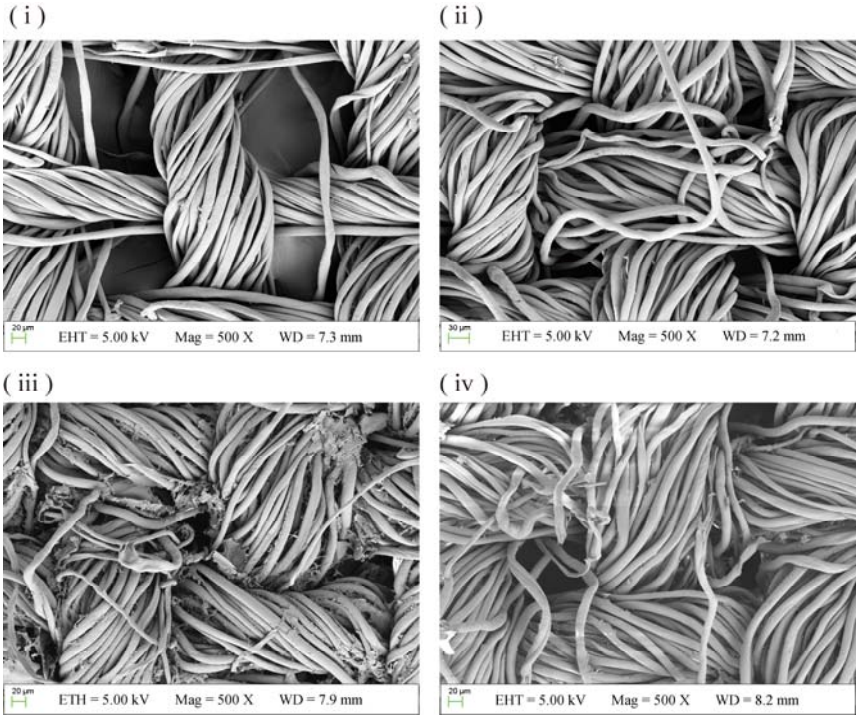

(B)

Figure 2

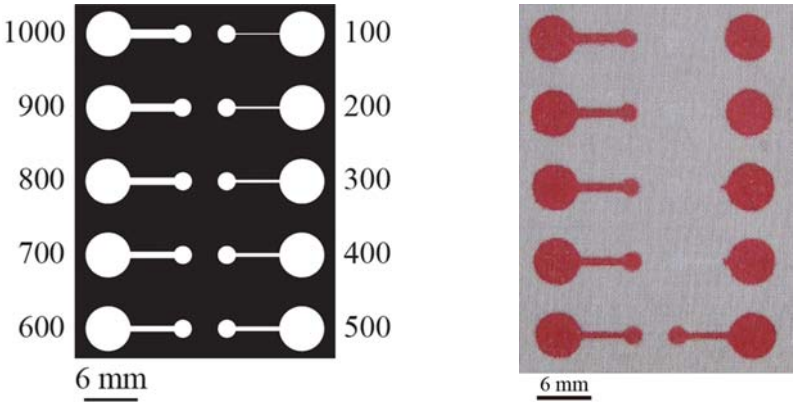

(A) **(B)**

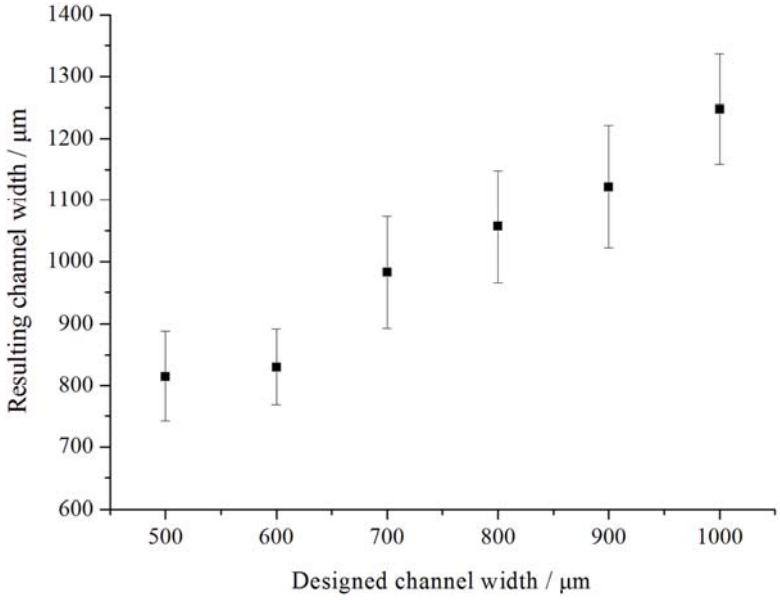

(C)

Figure 3

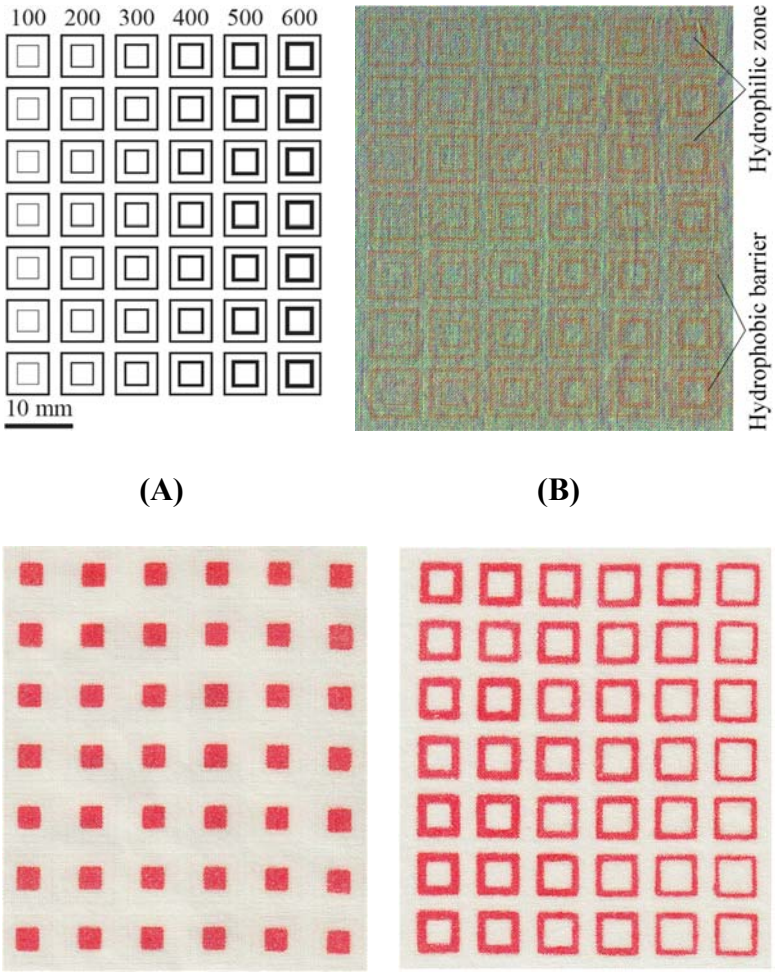

Figure 4

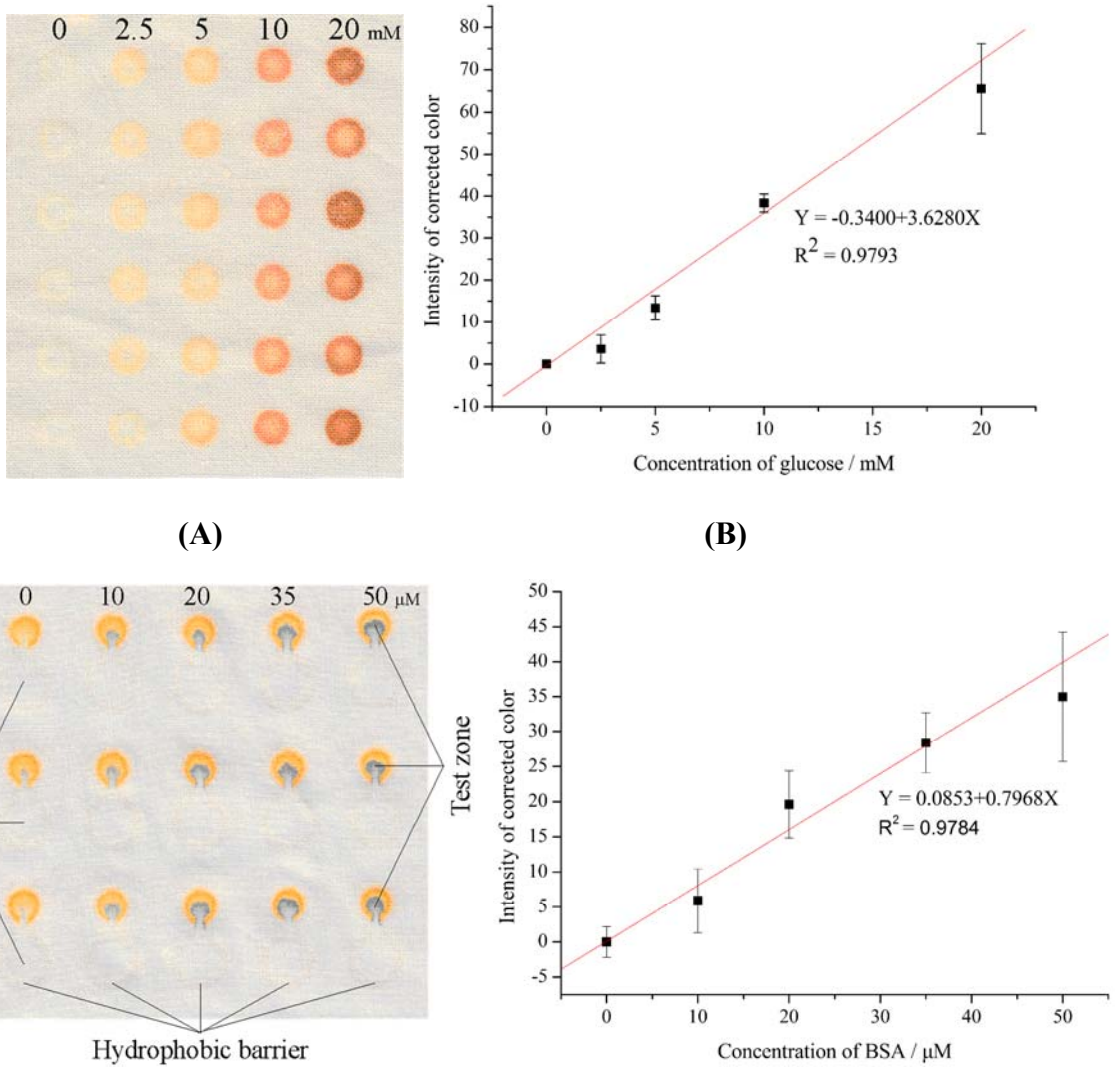

Figure 5